Chapter 6 Spin phonon coupling, giant dielectric constant and magneto-dielectric coupling in $BiFeO_3$-$TbMnO_3$ composite

6.1 Introduction

Bismuth ferrite (BFO) is the only multiferroic (MF) which shows both magnetic and electric ordering above room temperature (Neel temperature T_N = 643 K and ferroelectric Curie temperature T_C = 1100 K) [31, 34, 77]. BFO shows sizeable spontaneous polarization of order 10-100 μc/cm^2 due to Bi 6s^2 lone pair electrons [76]. On the other hand, the large magnetization is due to the Fe^{3+} spins causing the G-type antiferromagnetic ordering which is found to be canted in nature at room temperature in BFO with a spin cycloid period of 62 nm [35, 76]. The significant difference between ferroelectric Curie temperature and the Neel temperature which contributes to the low ME coupling has prompted many researchers to induce and improve the ME coupling in BFO by modifying the structure with doping of different rare earth materials like Sm, Dy etc. in small amount at bismuth sites [139, 140]. Moreover, the ME coupling of BFO has also been improved by preparing solid solutions with different rare earth manganites like $DyMnO_3$ and $PbTiO_3$,etc [67, 141]. The solid solutions of $RMnO_3$ and BFO provides a wide range of multiferroic properties due to the strain induced at the interface of the two materials which is quite high and also produces different coupling phenomena [67, 141]. The long-range antiferromagnetic spin order originated due to the competing magnetic interactions in these materials and lattice modulations due to magneto-elastic coupling are believed to be the origin of ferroelectric behavior in them. $TbMnO_3$ is highly studied and one of the most exciting MF materials of recent times for its strong magnetoelectric coupling [42, 141]. It has a distorted orthorhombic perovskite structure which should produce a significant strain on the rhombohedral lattice of BFO, opening possibilities for different interesting properties [144].These improved multiferroic properties like high dielectric constant, low loss and magnetoelectric coupling in the

materials are gaining attention nowadays for their application in many modern multifunctional devices like data storages systems, high energy capacitors, multiple state memory devices and Spintronics applications [84]. This has prompted us to prepare a composite consisting of BFO and $TbMnO_3$ and study its magnetic, transport, dielectric and ferroelectric properties in search of MD coupling along with other exciting phenomena like exchange bias, etc. Recently, it has also been shown by theoretical calculations and through experiments that ME behavior can be found in the systems in which spin-phonon coupling is present at the spin reorientation transition [141, 142]. In this context, we have prepared $BiFeO_3$-$TbMnO_3$ composite. In our earlier chapter it is found that the composite $BiFeO_3$-$TbMnO_3$ (7:3) showing enhancement in the magnetic property by manifold in comparison to pure $BiFeO_3$ and composites of BFO and TMO in other ratios. Hence, we present here our study on the structural, transport, dielectric, magnetodielectric and ferroelectric properties of composite $0.7BiFeO_3$-$0.3TbMnO_3$.

6.2 Experimental Techniques

The composite 0.7BFO-0.3TMO was prepared through the conventionalsolid-state reaction method as reported earlier [143]. X-ray diffraction pattern was recorded using an X-ray diffractometer (Model: Miniflex-II, Rigaku, Japan) with Cu Kα radiation (λ = 1.5406 Å) in step size of 0.002 with a scan speed of 2°/min. The surface morphology is studied from field emission scanning electron microscope (FESEM, Nova Nano SEM 450). Temperature dependent Raman spectra were taken in a Renishaw in Via spectroscope in the range of 200 cm^{-1} to 800 cm^{-1} using a 532 nm line of a diode pumped solid state laser delivering a power of 5 mW mm^{-2}. Dielectric measurements were carried out in a Keysight E4980A Precision LCR meter.

6.3 Results and discussion

6.3.1 Temperature-dependent Raman spectra analysis

Figure 6.1(a) shows the temperature dependent Raman spectra of the BFO-TMO composite spectra recorded in the temperature range of 80-300 K. We have also recorded the spectrum, for the pure BFO and pure TMO (not shown here) which shows the similar nature of the Raman spectra reported earlier [116, 141]. On the other hand, the composite material shows utterly different behavior with three broad peaks at ~ 300, 500 and 620 cm^{-1}. The peaks at ~ 620 $cm^{-1}$and 300 cm^{-1} are due to stretching and anti-stretching vibrations and the weak band ~ 500 cm^{-1} might be the bending vibration of Fe/MnO_6octahedron as reported in perovskite materials [144]. All the peaks in Figure 6.1(a) is seen to be shifted towards higher energy side down to 200 K and below 200 K softening of the band can be observed, i.e., band shifts slightly towards the lower energy side below 200 K. Raman modes should not show any kind of hardening or soften if only harmonic contributions are taken into account. In the anharmonic approximation usually, the Raman modes should harden on lowering the temperature and should approach plateau at lower temperature [145]. If both the stretching and anti-stretching mode shows hardening, then we can say that the anharmonicity dominates in the temperature dependent Raman spectra. Softening, i.e., decrease in the phonon frequency is usually observed in the case of phase change occurring in the structure, which is accompanied by a change of positions in the unit cell [144, 148]. The energy of the phonon is related to the anharmonicity as [147, 148].

$$\omega_{anh}(T) = \omega_0 - C\left(1 + \frac{2}{e^{\frac{\hbar\omega_0}{k_B T}} - 1}\right) \tag{6.1}$$

Where,ω_0 and *C* are adjustable parameters, T is the temperature, ħ is reduced Planck's constant and K is the Boltzmann's constant. In Figure 6.1(b) the red line shows the fitting of the phonon frequency of the stretching vibration ~ 620 cm^{-1} with Eq. 6.1. From Figure 6.1(b), it can be clearly seen that at higher temperature the phonon energies follow the anharmonic behavior and ideal anharmonic line deviates from the actual data points as soon as the temperature is decreased below 200 K. It is noteworthy to mention here that in the temperature dependent magnetization data an anomaly is found around 200 K that has been described as the spin reorientation transition [143, 144]. According to the mean field approximation when the long range magnetic ordering sets in a structure, it induces a renormalization of the phonon frequency [144, 146]. The phonon renormalization is found to be proportional to the spin-spin correlation function ($< S_i . S_j >$). The change in the phonon frequency due to this renormalization can be described as [147];

$$\delta\omega(T) = \omega(T) - \omega_{anh}(T) = K\left(\frac{M^2(T)}{M_0^2}\right) \quad (6.2)$$

Where, M_0 is the maximum value of magnetization. The difference of the two lines (fitted and recorded data) represents $\delta\omega(T)$. The inset of Figure 6.1(b) shows the variation of $\delta\omega(T)$ with temperature whereas the left panel shows a variation of $(M(T)/M_0)^2$ with temperature for both the bands. It is clearly observed that $\delta\omega(T)$ and $(M(T)/M_0)^2$ varies in a similar fashion; $\delta\omega(T)$ remains almost zero from room temperature to 210 K below which the value rises whereas the $(M(T)/M_0)^2$ drops down in magnitude below the spin reorientation transition temperature (~ 215 K). Thus, the relation between spins and the phonons in this structure is established.

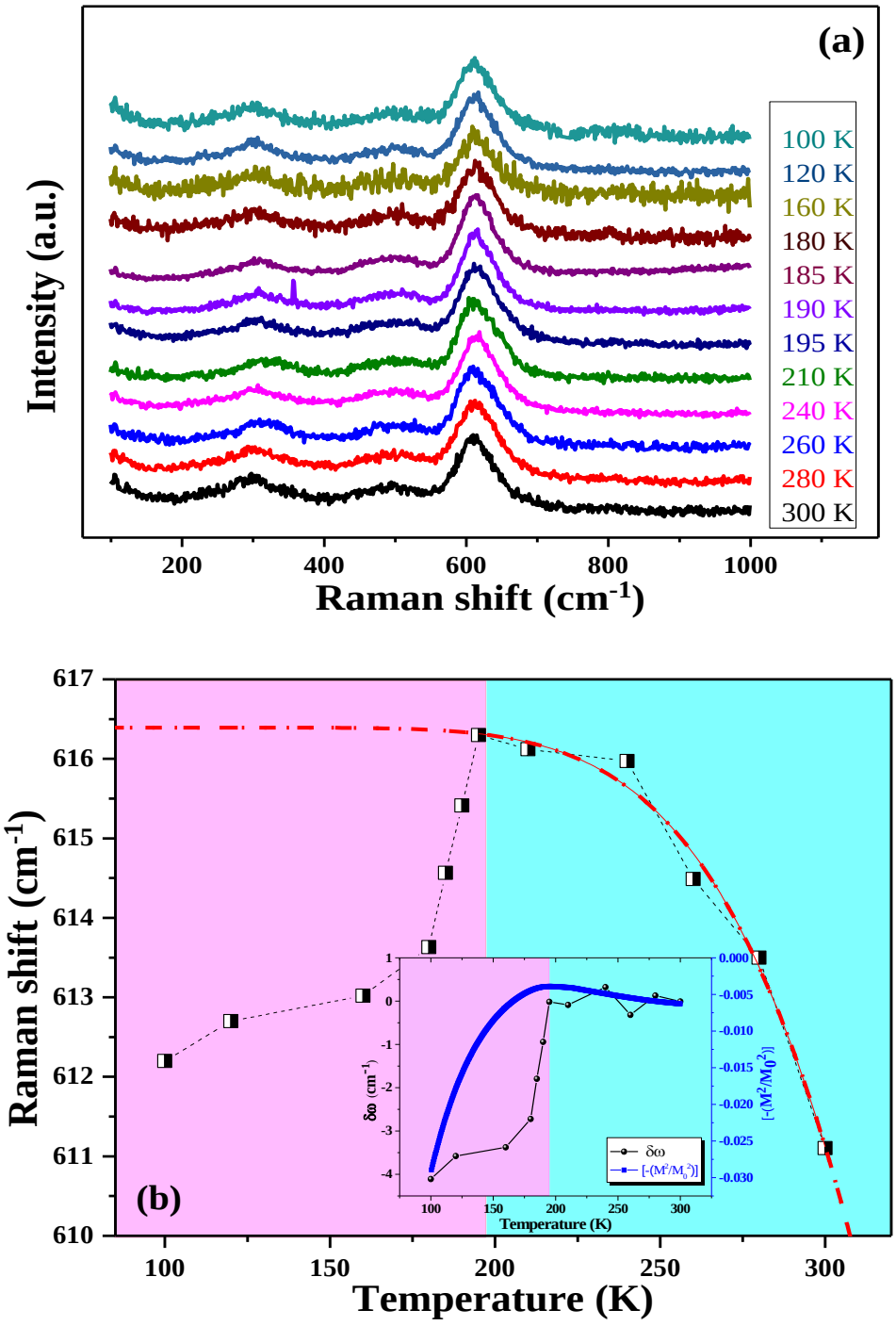

Figure 6.1 **(a)** temperature dependent Raman spectra of the BFO-TMO composite. **(b)** Variation of Raman shift of the stretching vibration with temperature. The red line shows the fitting according to **eq. 6.1.** Inset in figure 6.1(a) shows the x-ray diffraction pattern of the sample 0.7BFO-0.3TMO**.** Inset in figure 6.1(b) shows the variation of δω and $[-M^2/M_0^2]$ with temperature.

6.3.2 Dielectric analysis

The variation of the real part of dielectric constant (ε′) and the dielectric loss (tan δ) with temperature measured at different frequencies (1, 10, 50, 100, 500 KHz and 1 MHz) for the composite are shown in Figure 6.2. It is observed that at low temperature, the composite shows a low value of ε′ and above 200 K the values of constant dielectricreach up to 10^4 and show a plateau region over a wide frequency range which is very significant, since the behavior is expected for capacitor applications. At higher temperatures, the ε' shows strong frequency dependence. The low-temperature plateau which is the dispersionless region of the plot is understood to be from intrinsic contributions and the high-temperature regions are considered to be from a mixture of both contributions as there are dispersions in that regions [147]. Thus, the higher value of the dielectric constant at low frequencies can be considered as the contribution of all intrinsic and extrinsic contributions such as electronic, ionic, atomic and interfacial polarizations. However, above certain limiting frequencies of the applied field, only the electronic polarization comes into play in obtaining the value of the dielectric constant [148]. Moreover, the higher values of the dielectric constant and low value of loss (ε_r~ 30980 and tan δ ~1 at 1 KHz) at room temperature make the composite useful for capacitor applications. This is a significant increment achieved in the dielectric values of BFO based systems reported [149, 150].Pure BFO shows dielectric constant in the range 1600-1800 in the room temperature measured in same frequency range as reported by Ray et al, and Biswal et al, [149, 150]. Significant increase in the dielectric property is also achieved through doping of different rare earth materials such as, Dy, Sm and La etc. at the Bi site [139, 140] . Pure $TbMnO_3$ on the other hand shows high dielectric constant up to ~ 9000 in the same temperature range with a higher

loss value ~ 4-6 as reported by Wang et al, [49]. In case of thin film heterostructures like Au/$TbMnO_3$/$YBa_2Cu_3O_{7-x}$ on different substrates show low dielectric constant ~300-400 [43].

From Figure 6.2, it can be seen that the loss values also increase with increasing temperature and at a highertemperature, it shows peaks which shift to the higher temperature with increasing frequency. This type of frequency dependence is a common feature observed in rare earth manganites and BFO based systems and has been described as the signature behavior of relaxor ferroelectric [149, 150]. However, we are still unsure about the nature of the relaxation (whether Maxwell-Wagner type or Debye type).

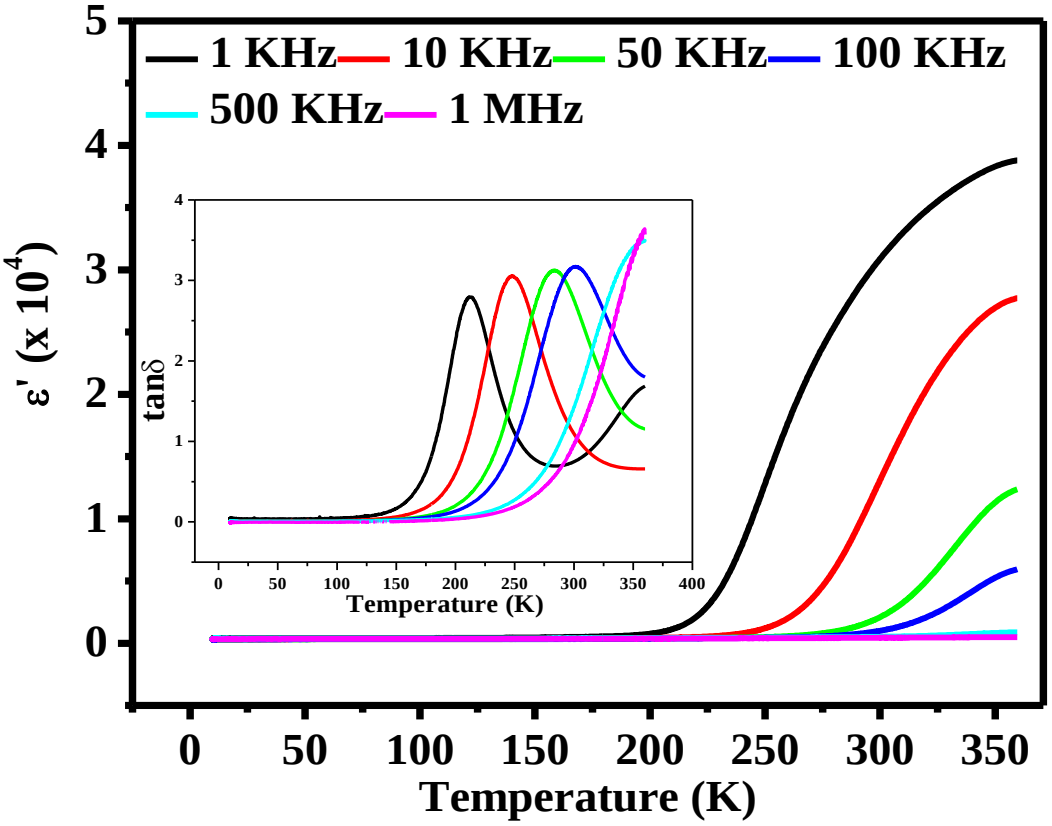

Figure 6.2 Temperature dependent real part of dielectric constant of BFO-TMO. Inset shows Variation dielectric loss with temperature.

6.3.3 Frequency dependence dielectric property

For that in Figures 6.3 (a) (b) and (c) we have presented the frequency dependence of ε′, ε″ and tan δ at different temperatures. A linear decrease in the ε″ with increasing frequency is signature behavior for the Maxwell-Wagner type relaxations whereas for the case of Debye relaxations; the frequency dependence vanishes [152]. In Figure 6.3(b), it can be found that Maxwell-Wagner does not completely satisfy the data, especially at the mid-frequency region where a plateau region can be found indicating multiple relaxation mechanisms. We tried to fit the data with a modified version of the Maxwell-Wagner model where Debye contributions were also included. The data fit well with the modified version suggesting Debye contributions to be there in addition to the dominating Maxwell-Wagner contributions. Such dielectric behavior with contributions from Debye and non-Debye relations have been previously reported in different perovskite systems including BFO based systems [150].

6.3.4 Magneto-Dielectric (MD) analysis

We have performed the magneto-dielectric behavior at an applied magnetic field of 0-1.4 T with 1 kHz as the measuring frequency from 9 to 285 K [shown in Figure 6.3(d)]. The difference between the two lines (i.e., with and without field) clearly shows the presence of magneto-dielectric coupling. The MD coefficient can be calculated using the relation;

$$\% MD = \frac{\varepsilon'(H)-\varepsilon'(0)}{\varepsilon'(0)} \times 100 \quad (6.3)$$

Where, $\varepsilon'(H)$ and $\varepsilon'(0)$ are the dielectric constant at an applied magnetic field H and at zero applied field. It can be seen from the plot that the sample magneto-dielectric behaviour in the

temperature ranges 240-260 K with maximum being at 250 K. At 250 K a maximum 3% MD coupling can be seen at measuring frequency 1 kHz which is shown in the inset of Figure 6.3(d). Generally, positive and negative MD coupling has been ascribed to the influence of the applied magnetic field on the dipolar relaxation of the material. Although the origin of the magnetoelectric coupling in a material is still not very clear, there are many models explaining the phenomenon. Few reports are there where magneto-striction and piezo-striction are held responsible for the observed magnetoelectric coupling [67, 141]. One may confuse the intrinsic magnetoelectric coupling with the one arising from the space charge polarization which is extrinsic in nature. In general, interfacial space charge polarization gets suppressed on the application of a magnetic field due to the Lorentz force acting on them giving rise to the change in dielectric constant. In a layered structure with multiple interfaces, the mismatch between the lattice constants or the work functions of the layers can also create strong magneto dielectric behaviour which is not intrinsic in nature [67]. The negative intrinsic MD coupling can simply be understood to be due to strain induced on the piezoelectric which arises in the system by the application of the magnetic field [67, 144]. This generates an electric field which can influence the polarization of the system leading to a decrease in the dielectric permittivity. The positive MD behaviour on the other hand is more critical to explain and is rare to be found also. Earlier the positive MD effects were linked to the magnetoresistance and the Maxwell-Wagner relaxations [51]. Recently, it has been found in perovskite manganites where the phenomenon were described to be intrinsic in origin as the correlation between the magnetic and the dipolar ordering was held responsible for the observed phenomenon [51]. Positive giant MD behaviour

has been observed in Sm and Er doped BFO nanoparticles and was explained on the basis of strain developed due to lattice mismatch and magneto-striction effects.

Recently, Palakkal et al, have shown large positive and negative magnetodielectric coupling in their La_2NiMnO_6 and $La_2NiFe_{0.5}Mn_{0.5}O_6$ systems which they explained on the basis of the influence of magnetic field on the intrinsic dipolar relaxations. The MD effects in our case have been found in the temperature range where the dipolar relaxation occurs (i.e., around 250 K) indicating correlations between the dipolar relaxation and the magnetic ordering. From our temperature dependent dielectric, impedance study and frequency dependent dielectric study at the different temperature, we have found that both Maxwell-Wagner and intrinsic Debye type relaxations are present in our system. Thus to clear the air about the origin of the observed MD behaviour in our sample we, rely on the temperature dependent Raman study. From the temperature dependent Raman study (Figure 6.1) we have found that in the system, the spin and phonon couple near the spin reorientation temperature [143]. The spin reorientation transition in the system is very close to the dielectric relaxation temperature of the system where the MD behaviour has been found. There is a finite possibility that the MD behaviour is arising in the system due to the magneto-structural interaction. Similar feature was observed in the case of La_2CoMnO_6 where at the magnetic ordering temperature spin phonon coupling as well as the MD behaviour was found to exist [143].

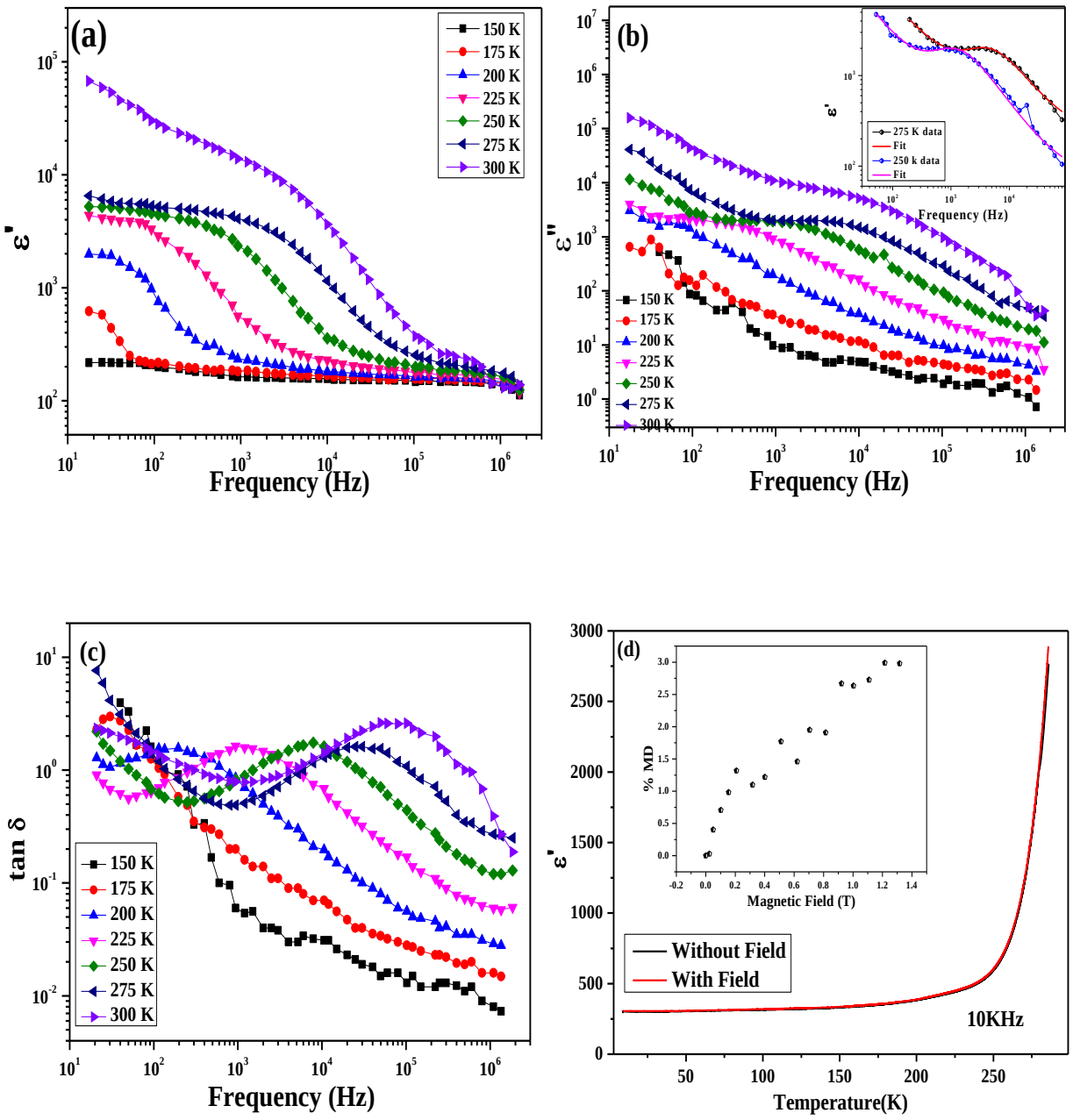

Figure 6.3. Variation of **(a)** ε' **(b)** ε'' and **(c)** tanδ with frequency of the composite BFO-TMO. **(d)** Variation of real part of dielectric constant with and without magnetic field**.** Inset in**(b)** shows ε'' variation of frequency fitted with an equation consisting both Debye and Maxwell-Wagner contribution. Inset in **(d)** shows Variation of % MD with magnetic field at 250 K and measuring frequency 1 kHz**.**

6.3.5 Impendence spectroscopy analysis

To further support our dielectric results that both Debye and non-Debye processes take part in the dielectric behaviour we have performed the impedance measurements at different temperatures (200, 225, 275 and 300 K) thus also studying the evolution of different processes with temperature. The real and imaginary components of complex impedance are plotted in the Nyquist or Cole-Cole plot for different temperatures [Figure 6.4(a-d)]. Different contributions can be seen as different semi-circular arcs in the Cole-Cole plot. The overall impedance can be considered to be result of two parallel combinations of resistance and capacitance connected in series arising from the grain and grain boundary contributions [inset of Figure 6.4(b)] [150]. The contribution from grain boundary is considered to be dominated by the space charge polarisation whereas the grain contribution is dominated by the intrinsic dipolar relaxation. The impedance can be written as [150];

$$Z(f) = \frac{R_G}{1+R_G Q_G (2\pi f)^{\alpha_1}} + \frac{R_{GB}}{1+R_{GB} Q_{GB} (2\pi f)^{\alpha_2}} \quad (6.4)$$

Where, the suffix G and GB represent grain and grain boundary, R is the resistance and Q is the capacitance. α_1 and α_2 are fitting parameters whose deviation from unity indicates presence of non-Debye relaxation process. At 300 K two suppressed semi-circular arc can be observed in the plot with arc centres below the real axis signifying distributed elements in the relaxation process [149]. From the suppressed nature of the arcs it is confirmed that there are non-Debye contributions in the relaxation process. Two semicircles can be seen from the plot corresponding to grain and grain boundary contributions to the impedance. Interestingly it can be observed that the contribution from grain boundary diminishes as we decrease the temperature. At 200 K only

one semicircle can be seen which signifies that at low temperature the grain contribution dominates in the impedance spectrum. The Nyquist plots are fitted with eq. 6.4 and the values obtained from the fitting clearly indicate to the presence of Debye and non-Debye process involved in the relaxation phenomena at higher temperatures. However, at low temperatures only Debye type relaxation can be found.

The two semicircles in the Cole-Cole plots have been ascribed to the contribution arising from grain and grain boundary of the material in several reports. However, in a recent report Biswal *et al*, explained two semicircles in their Cole-Cole plot to be arising from the contributions from different phases (*R3c* and *Pbnm*) present in their sample [149]. In our case, although there are different phases (BFO in *R3c* and *Pbnm* phases and TMO in *Pbnm* phase), two semicircles in the plot is not due to different phases present in our sample as the structure remains the same throughout the temperature range studied in contrast to the Cole Cole plots which change with decreasing temperature. The changes are due to immobile charges and temperature dependent vacancies. Moreover, in the FESEM micrograph, clear grain and grain boundary can be seen which supports the assumption that the circles in the Cole-Cole plots arises due to grain and grain boundary in the composite.

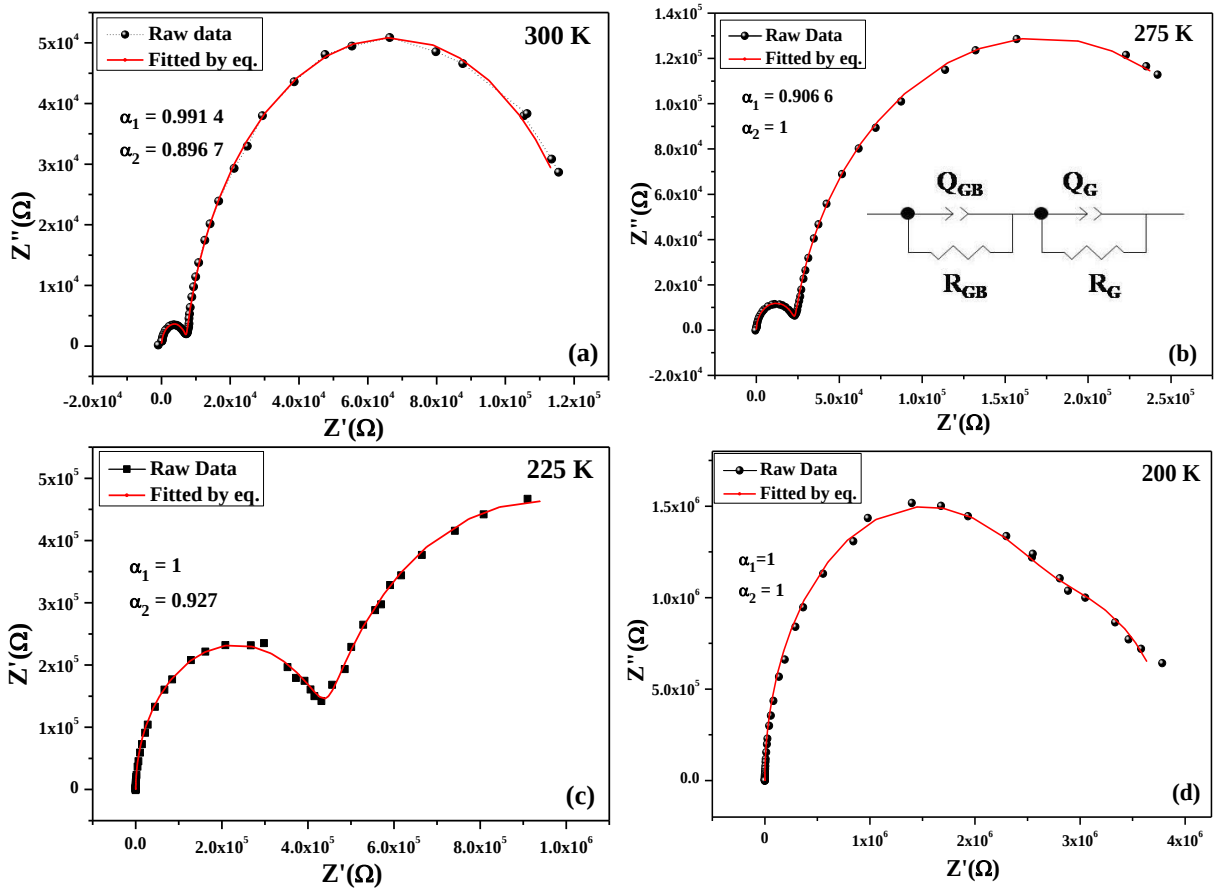

Figure 6.4. Typical impedance plot (Cole-Cole plot) of BFO-TMO composite at **(a)** 300 K **(b)** 275 K **(c)** 225 K and **(d)** 200 K. The red lines in the plots show the fitting of the data as per **eq. 5.** The equivalent circuit is shown in **(b).**

6.4 Conclusion

Here in this chapter, we have investigated the MD and magneto-structural behavior of the multiferroic composite 0.7BFO-0.3TMO. The anomalous softening of the phonon modes indicated toward a possible spin-phonon coupling. The similarity in the deviations of the phonon energy from the anharmonicity (T) and the $M^2/M_0^2(T)$ confirmed the presence of spin-phonon coupling near the spin reorientation temperature (T*). The relaxation peaks were found in the relaxor type dielectric behavior which was dominated by Maxwell-Wagner type relaxations near the room temperature. The contribution of intrinsic Debye relaxations and MW relaxations

arising from the accumulated space charge near the interfaces of the two materials were separated from the dielectric vs. frequency measurements where low frequency and high temperature contributed to the MW relaxations while the high frequency and low-temperature regions were dominated by the intrinsic Debye relaxations. Significant magnetic field dependence of the dielectric constants was observed (3% MD coupling) which we explain on the basis of a few factors such as, the magneto-structural coupling, Maxwell-Wagner contributions, etc.